Sio-Iong Ao
Haeng-Kon Kim
Mahyar A. Amouzegar *Editors*

Transactions on Engineering Technologies

World Congress on Engineering and Computer Science 2019

Springer

Transactions on Engineering Technologies

Sio-Iong Ao · Haeng-Kon Kim ·
Mahyar A. Amouzegar
Editors

Transactions on Engineering Technologies

World Congress on Engineering and Computer Science 2019

Springer

Editors
Sio-Iong Ao
IAENG Secretariat
International Association of Engineers
Hong Kong, Hong Kong

Haeng-Kon Kim
School of Software Convergence
Daegu Catholic University
Daegu, Korea (Republic of)

Mahyar A. Amouzegar
Provost and Senior Vice-President
University of New Orleans
New Orleans, LA, USA

ISBN 978-981-15-9208-9 ISBN 978-981-15-9209-6 (eBook)
https://doi.org/10.1007/978-981-15-9209-6

This Springer imprint is published by the registered company Springer Nature Singapore Pte Ltd.
The registered company address is: 152 Beach Road, #21-01/04 Gateway East, Singapore 189721, Singapore

Preface

A large international conference on Advances in Engineering Technologies and Physical Science was held in San Francisco, California, USA, October 22–24, 2019, under the auspices of World Congress on Engineering and Computer Science (WCECS 2019). WCECS 2019 is organized by the International Association of Engineers (IAENG). IAENG, originally founded in 1968, is a non-profit international association for engineers and computer scientists. The WCECS Congress serves as an excellent platform for the members of the engineering community to meet and exchange ideas. The Congress in its long history has found the right balance between theoretical and application development, which has attracted a diverse group of researchers, leading its rapid expansion. The conference committees have been formed with over two hundred members including research center heads, deans, department heads/chairs, professors, and research scientists from over 30 countries. The full committee list is available at the congress' website: www.iaeng.org/WCECS2019/committee.html. WCECS conference is truly an international meeting with a high level of participation from many countries. The response to the WCECS 2019 conference call for papers was outstanding, with more than three hundred manuscript submissions. All papers went through a rigorous peer-review process and the overall acceptance rate was 51%.

This volume contains 14 revised and extended research articles, written by prominent researchers, participating in the congress. Topics include chemical engineering, electrical engineering, computer science, manufacture engineering, and industrial applications. This book offers the state of the art of tremendous advances in engineering technologies and physical science and applications; it also serves as an exceptional source of reference for researchers and graduate students working with/on engineering technologies and physical science and applications.

Hong Kong, Hong Kong — Sio-Iong Ao
Daegu, Korea (Republic of) — Haeng-Kon Kim
New Orleans, USA — Mahyar A. Amouzegar

Contents

A Simplified Analytical Approach on the Dynamic Pressures in Cylindrical Vertical Tanks

Frank Otremba, Robert Hildebrand, José A. Romero Navarrete, and Christian Sklorz

Abstract A simplified methodology is proposed to estimate the dynamic pressures developed within partially filled cylindrical vertical tanks when subjected to earthquake-related horizontal accelerations. The total pressure at the bottom of the tank is calculated as the superposition of vertical and horizontal pressures. While the magnitude of the vertical pressure depends on the free surface height of the liquid, the horizontal pressure depends on the magnitude of the horizontal acceleration and on the diameter of the tank. The liquid free surface oscillation angle is simulated based upon the principles of the simple pendulum analogy for sloshing. The length of the pendulum, however, is set on the basis of a methodology to calculate the free sloshing frequency of partially filled containers. Such a methodology is experimentally verified in this work. The outputs of the model for full-scale situations suggest that the lateral perturbation—sloshing phenomenon (earthquake effect) can generate an increase in the total pressure of 56% above the no lateral perturbation situation, further suggesting that such an overpressure should be taken into account when designing tanks that could be potentially subjected to earthquake-related perturbations.

Keywords Experimental approach · Hazmat · Pendulum analogy · Sloshing · Transition matrix approach · Vertical cylindrical tanks

F. Otremba · J. A. Romero Navarrete (✉) · C. Sklorz
Federal Institute of Materials Research and Testing (BAM), Unter den Eichen 87, 12205 Berlin, Germany
e-mail: jose-antonio.romero-navarrete@bam.de

F. Otremba
e-mail: frank.otremba@bam.de

C. Sklorz
e-mail: christian.sklorz@bam.de

R. Hildebrand
Lake Superior University, 650 W Easterday Avenue, Sault Ste. Marie, MI 49783, USA
e-mail: rhildebrand@lssu.edu

S.-I. Ao et al. (eds.), *Transactions on Engineering Technologies*,
https://doi.org/10.1007/978-981-15-9209-6_1

1 Introduction

Sloshing in tanks is the result of perturbations associated to normal or extraordinary operating conditions [1]. The consequences of such a motion of the liquid depend on the type of container involved, whether it is a transport container or a fixed container [2]. In the case of a road transport container, for example, the different maneuvers and the pavement roughness are the sources of perturbation for the liquid cargo [3]. In the case of fixed containers, the sloshing sources derive from environmental factors, such as the wind conditions [4], or from soil movements [5, 6]. Sloshing in such fixed facilities can originate spill issues as well as potential overpressures on the tank material due to the combination of dynamic pressures [7, 8]. In this respect, the low frequency of the earthquake-related oscillations can be in the range of the natural sloshing frequencies of such facilities [9]. However, to assess the potential effect of the earthquake motion on the stresses developed within the tank wall's material, it is necessary to analyze the magnitude and frequency of the perturbation. That is, to analyze the dynamic response of the contained liquid to the perturbation accelerations. In this paper, a simplified methodology is proposed to estimate the potential effect of the earthquake accelerations on the dynamic pressures developed at the bottom of full-scale tanks, as a function of both the diameter of the tank and its fill level. This paper is based upon a WCECS 2019 Conference paper [10].

2 Theoretical Modelling Fundamentals

For rectangular containers, there is a validated formulation to predict the free sloshing frequencies of the contained liquids, which is based upon the principles of gravity waves, according to the following formulation [11]:

$$\lambda\left(\frac{\omega}{2\pi}\right) = \sqrt{\left(\frac{g\lambda}{2\pi}\tanh\left(\frac{2\pi}{\lambda}h_l\right)\right)} \tag{1}$$

where h_l is the depth of the rectangular container; ω is the angular sloshing frequency; and λ is the wavelength $= 2\ L$, where L is the liquid's free surface length. The relationship between the natural sloshing frequency f in Hertz, and ω (rad/s) is given by $\omega = 2\pi f$. However, this formula has been validated for nonrectangular tank shapes, by considering an equivalent height h_e for an equivalent rectangular container. This is illustrated in Fig. 1, in the case of a half-filled circular cross-section tank. The validation for circular and elliptical shapes has been reported in [12]. In the case of the illustration in this figure, the half circular area of diameter D is substituted by a rectangular shape having the same area and the same free length, but with a depth that is calculated for having the same area, that is:

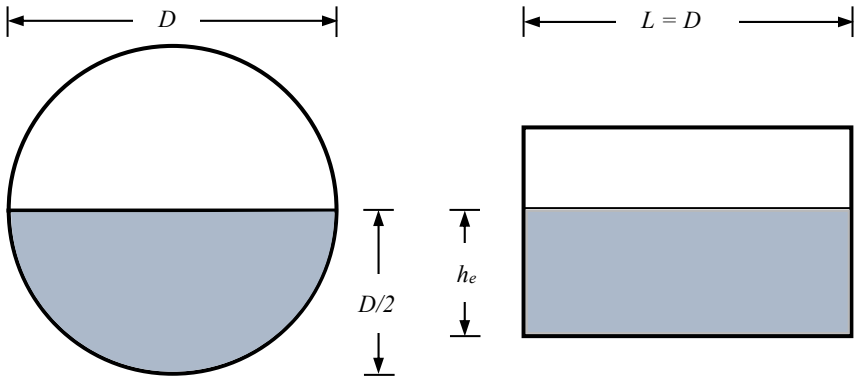

(a) Half-filled circular tank (b) Equivalent rectangular container

Fig. 1 Equivalent liquid depth for the calculation of the natural sloshing frequency with Eq. (2)

$$h_e = \frac{\pi D^2}{8L} = \frac{\pi D}{8} \tag{2}$$

In the case of a vertical cylindrical tank, there would be several possibilities to choose a significant diameter representing the free length L of the liquid. For example, it could be an average diameter, or the maximum diameter. That is, there would an unlimited number of possibilities to choose such a length, as it varies from zero at the container's wall, to a maximum length at the diameter.

3 Experimental Setup

The aim with the testing rig was to verify the natural sloshing frequency formulation (Eq. (1)). For that purpose, three container shapes were considered: rectangular, conical, and cylindrical. In the case of the conical and circular tank shapes, there was the prominent interest of identifying a significant diameter for such formulation.

Concerning the horizontal perturbation of the partially filled tanks, several methods were possible, including a horizontal shaking table on which the tank were set, or a horizontally impacted wheeled vehicle on which the tank was set. Because of an existing instrumented testing device, the second perturbation possibility was considered, which was instrumented with strain gages at the position of each of the four vehicle's wheels. For moving the vehicle toward the moderate impact surface, there were also different operational principles to select, including the use of a tilted surface on which the vehicle would move due to gravity, or to pull the vehicle through a string attached to a falling mass. The second possibility was chosen for moving the vehicle with the tank, as the tilt table would affect the free sloshing length due

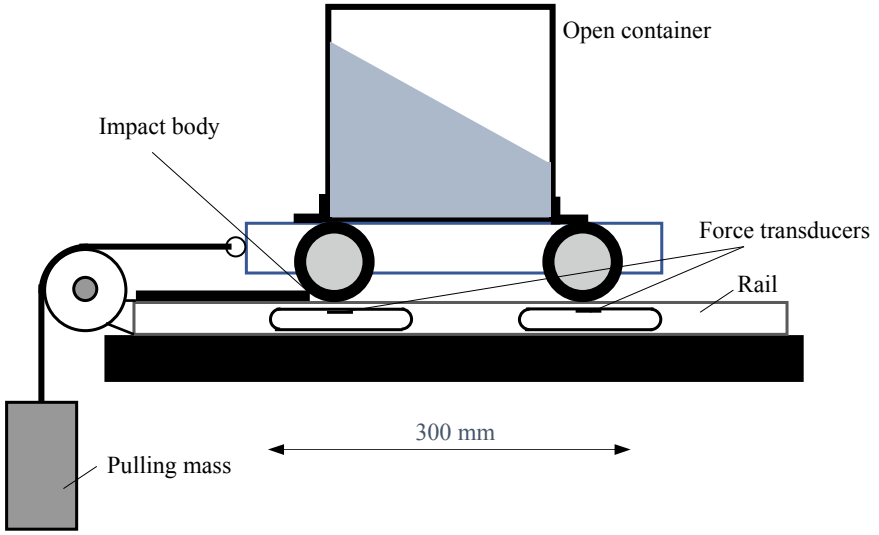

Fig. 2 Experimental setup to horizontally perturb a partially filled container

to the associated slope, which would interfere with the free sloshing of the liquid in the tanks. Different falling masses were considered so as to keep a moderate impact condition on the vehicle-tank system. Figure 2 illustrates the layout of the testing facility, which was instrumented with strain gages, adhered to the supporting rails that guided the vehicle. The working fluid was tap water.

4 Formulation Verification Data

Figure 3 illustrates the three shapes that, under the perspective of the testing rig described in the previous section, were tested for verification of the gravity wave formulation of Eq. (1). In the case of the rectangular container, the perturbation was along the longitudinal axis, involving a free surface length of 185 mm. For the tanks of circular cross-section, preliminary tests revealed that the significant length for applying Eq. (1) was the diameter of the liquid's free surface. Such an output is attributed to the larger freedom to move of the liquid at such larger dimension. Furthermore, in the case of the conical tank, two diameters were considered for verification. One was an average diameter for the full height of the liquid, and the other one, the maximum diameter for that full height of the liquid.

As an example of the data obtained for analysis, Fig. 4 illustrates the time history for a selected strain-gaged force transducer, in terms of the strain, in the case of the rectangular tank with a liquid height of 142 mm. It can be observed in these data that the signals correspond to the approaching of the car to the obstacle, the consequential impact; the rebound of the vehicle from the impact, and the residual sloshing once the

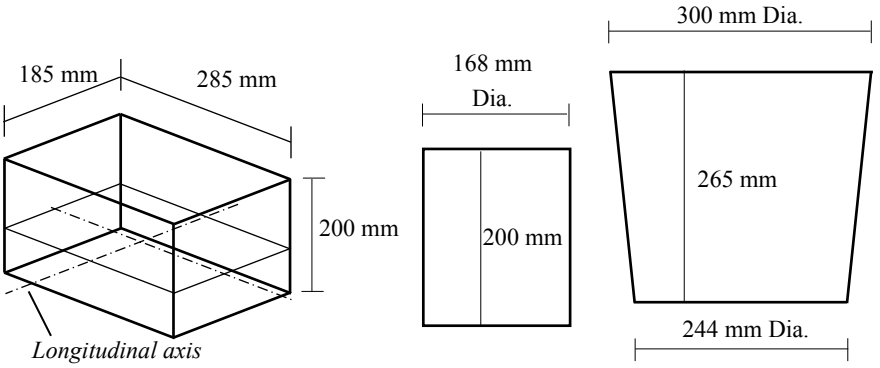

Fig. 3 Three tank shapes for assessing the gravity waves formulation of Eq. (1)

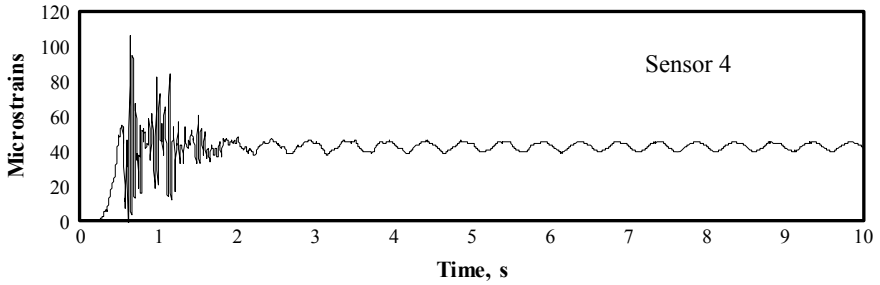

Fig. 4 Strain signal for the rectangular tank at 142 mm liquid's height

vehicle wheels stabilize in their position. The analysis for checking the validity of the gravity waves approach will thus consider the signals acquired during the residual sloshing time segment. Figure 5 depicts the theoretical and experimental results for the free sloshing frequencies, as a function of the tank's shape and liquid's height. As it was mentioned above, for the conical tank (part (b) of this figure), two different diameters were considered: the average (avr) and the maximum (max) for the considered height of the liquid. For these data, Table 1 lists the discrepancy in percentage, between the theoretical and the experimental data, suggesting certain influence of both the tank shape and the tank level, on the magnitude of such discrepancy, ranging from 0.03% (Conical Avr), to a maximum of 10.34% (Conical Max). The bottom row of this table lists the average values for the discrepancies, revealing that the ranking of validation from the best to the worst is as follows: rectangular tank, average conical, cylindrical and maximum conical. These results are considered acceptable in general terms, so that the gravity waves formulation will be used to simulate the sloshing in full-size tanks.

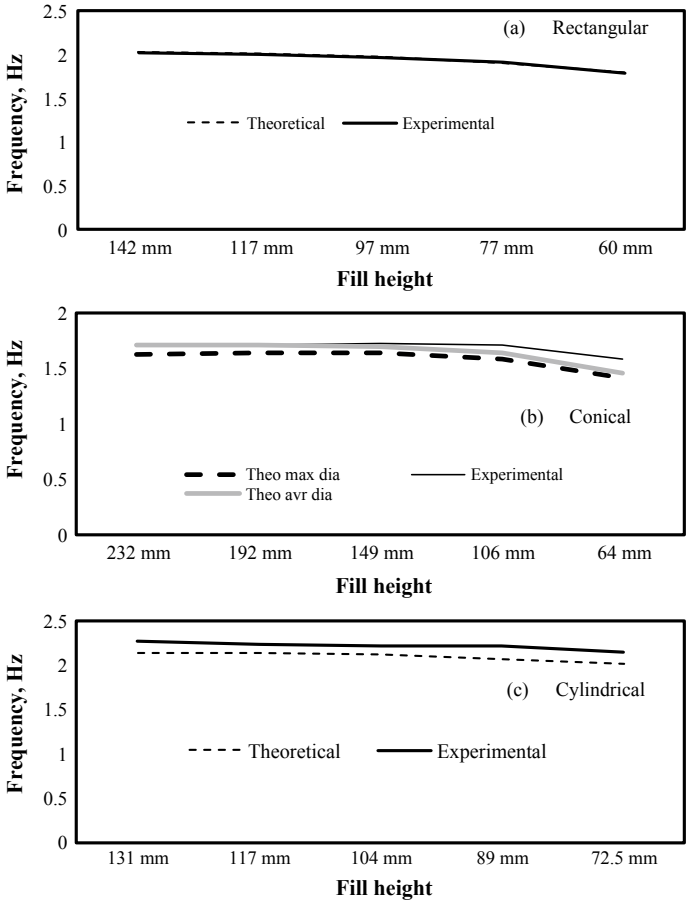

Fig. 5 Theoretical and experimental values for the free sloshing frequency as a function of the fill height and tank shape

Table 1 Difference between the experimental and the theoretical data (%)

Height (mm)	Conical Max	Conical Avr	Height (mm)	Rectangular	Height (mm)	Cylindrical
232	5.00	0.03	142	−0.69	131	5.83
192	4.50	0.24	117	−0.21	117	4.66
149	5.57	1.85	97	−0.97	104	4.93
106	7.41	4.24	77	0.71	89	6.52
64	10.34	7.92	60	−0.92	72.5	6.97
	6.56	2.85		−0.41		5.78

5 Simulation Approach and Results

The gravity waves formulation will be used to simulate the dynamic pressure at the bottom of a partially filled full-size tank, throughout the incorporation of a simple pendulum to describe the first mode liquid's sloshing [9], where the length of such simple pendulum will be based upon the natural sloshing frequencies obtained from the gravity waves approach. According to such simplified approach, the slope of the free surface will correspond to the swing angle of the simple pendulum. Figure 6 describes this situation, where the lateral acceleration a_L due to an earthquake, is illustrated. The parameters considered for the simple pendulum motion include its length L_p and its mass m_p.

The dynamic response of the simple pendulum is obtained through the Transition Matrix Approach, involving a Taylor's expansion for the free response, and a Convolution Integral for the particular response, as described in [13]. The pressure at the bottom of the tank is thus calculated as the superposition of the vertical pressure p_v due to gravity, as a function of liquid density ρ and height h, and the horizontal pressure p_h, as a function of the length L of the vessel (diameter D), the acceleration a_L, and of the liquid density ρ, as follows:

$$p_v = \rho\, g\, h \tag{3}$$

$$p_h = \rho\, a_L\, D \tag{4}$$

Sixteen different commercial vertical cylindrical tanks are considered to simulate the potential effect of earthquake-related accelerations on the magnitude of the pressure at the bottom of such tanks, partially filled at 75, 50 and 37.5%. The tank's full height H and the diameter of such commercial tanks are described in Fig. 7 [14], involving a wide variation of dimensional characteristics, with capacities ranging from 100 to 50,000 m^3; diameters ranging from 4.73 to 60.7 m; while the total height of the tanks ranges from 6 m in the case of the smaller tank, to 18 m in the

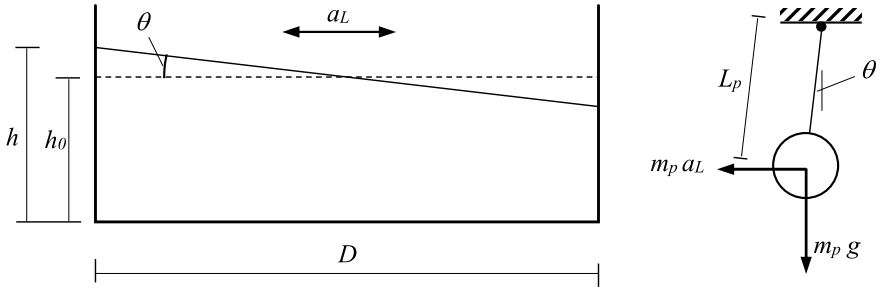

Fig. 6 Analogy approach between the free surface of the liquid and the swing angle of a simple pendulum. g is the gravity acceleration (9.81 m/s^2)

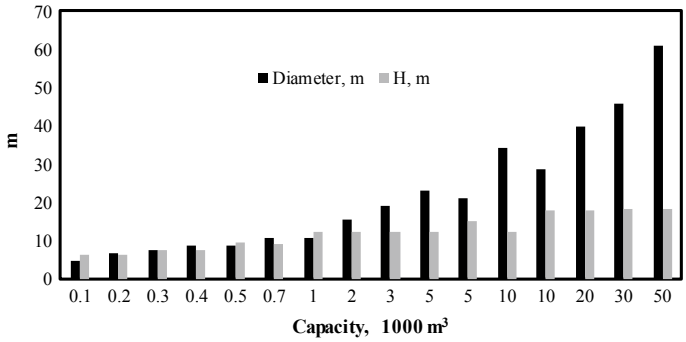

Fig. 7 Information of diameter and full height of commercial tanks. Own, with data from [14]

case of the largest one. Considering the 3 fill levels of interest, a total of 48 simulation conditions exist, covering a full range of tank's operational and design situations. Such conditions are listed in Table 2, including the initial height h_0 for the liquid and the resulting pendulum length L_p for the selected partial fill levels. In these data and in general terms, the length of the pendulum increases when the fill level decreases, thus involving lower natural sloshing frequencies. On the other hand, increasing the

Table 2 Simulation conditions, including the initial liquid height h_0 and the simple pendulum length L_p, as a function of the tank diameter D

D (m)	h_0 75% (m)	h_0 50% (m)	h_0 37.5% (m)	L_p 75% (m)	L_p 50% (m)	L_p 37.5% (m)
4.73	4.50	3.00	2.25	1.51	1.56	1.66
6.63	4.50	3.00	2.25	2.17	2.37	2.68
7.58	5.63	3.75	2.81	2.46	2.64	2.93
8.45	6.94	4.63	3.47	2.72	2.87	3.13
8.53	5.63	3.75	2.81	2.80	3.08	3.50
10.43	6.75	9.00	4.50	3.43	3.35	3.79
10.43	6.00	3.38	4.50	3.50	4.32	3.79
15.18	9.00	6.00	4.50	5.07	5.71	6.61
18.98	9.00	6.00	4.50	6.69	7.96	9.56
20.9	11.25	7.50	5.63	7.12	8.21	9.66
22.8	9.00	6.00	4.50	8.58	10.69	13.17
28.5	13.43	8.95	6.71	10.06	12.00	14.42
34.2	9.00	6.00	4.50	16.04	21.71	27.82
39.9	13.35	8.90	6.68	16.23	21.00	26.35
45.6	13.50	9.00	6.75	19.86	26.33	33.43
60.7	13.50	9.00	6.75	32.01	44.43	57.54

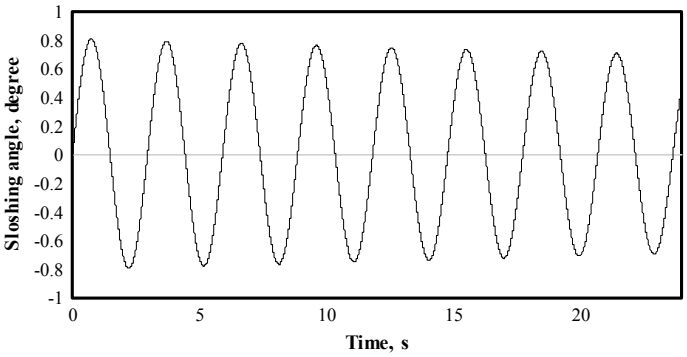

Fig. 8 Free response of the liquid surface sloshing for a 6.63 m diameter tank, at 75% fill level

diameter of the tank produces larger pendulum lengths, with the consequential reduction in the values of the natural sloshing frequencies. The working fluid in this case will be considered a hazardous material, which is a common commodity in these cases, with a density of 748.9 kg/m^3 (gasoline).

The outputs of the model will be presented in the following four stages:

(i) a sample of the free response of the sloshing phenomenon.
(ii) a sample of the time histories for a given simulation condition, of the sloshing angle variations and the respective pressure at the bottom of the tank when it is subjected to a horizontal earthquake-related acceleration.
(iii) the overall time response of the full set of testing conditions in order to analyze the effect of the different parameters, on the maximum pressures attained at the bottom of the respective tanks.
(iv) the outputs for the higher fill level considered, aiming at analyzing the absolute increase in the pressure at the bottom of the tank, due to the liquid sloshing-lateral perturbation phenomena.

Figure 8 illustrates a sample time variation of the sloshing angle for a specific tank shape and fill level, where a very low damping constant was considered for the pendulum, in view of the experimental measurements illustrated in Fig. 4.

The time variation of the horizontal acceleration due to an earthquake during a five-second time span, is illustrated in Fig. 9, suggesting a range of low excitation frequencies having a maximum magnitude of 1.3 m/s^2.

Figure 10 illustrates a sample of the sloshing angle and the developed pressures at the bottom of the tank referred in Fig. 8, when it is subjected to the horizontal acceleration pattern described in Fig. 9. According to these results, a maximum slosh angle of 2° is attained. On the other hand, the vertical pressure exhibits a very small variation, when it is compared with the horizontal component counterpart.

To identify the potential relationships between the tank properties/operating conditions and the magnitude of the pressure attained at the bottom of such tank when subjected to the 5-second accelerations illustrated in Fig. 9, the 48 simulating

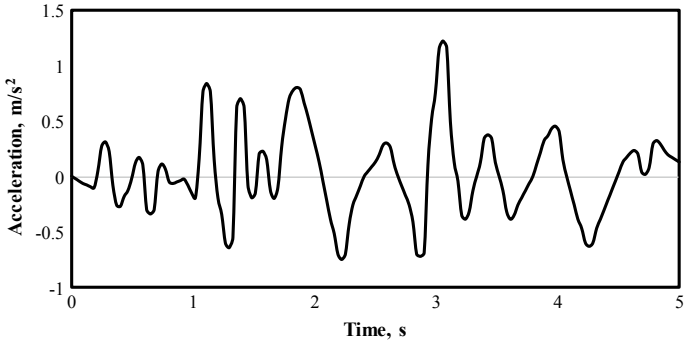

Fig. 9 Earthquake-related horizontal acceleration time variation. *Source* Own, with selected data from [15]

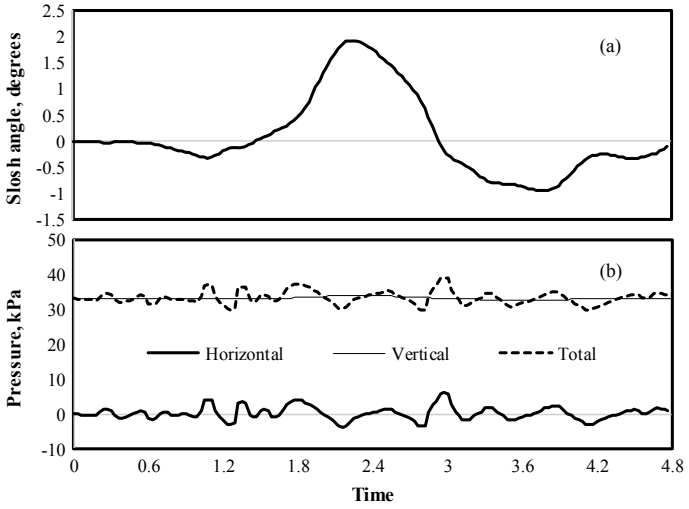

Fig. 10 Time histories for the free surface angle and the different pressures at the bottom of a 6.63 m diameter tank, at 75% fill level, when subjected to the horizontal acceleration in Fig. 9

conditions listed in Table 2 were sequenced, and the results put together in the respective graphs, in terms of simulation instants, 0.03-second apart. The different parts of Figs. 11 and 12 illustrate such outputs, including the slosh angle, the different pressures, as well as the earthquake effect (EE), calculated as the ratio of the maximum value of the dynamic pressure and the static pressure (in %). These outputs suggest the following:

– The maximum slosh angles occur for the smaller tank diameters, attaining a maximum magnitude of 2.5° (part (a), Fig. 11).

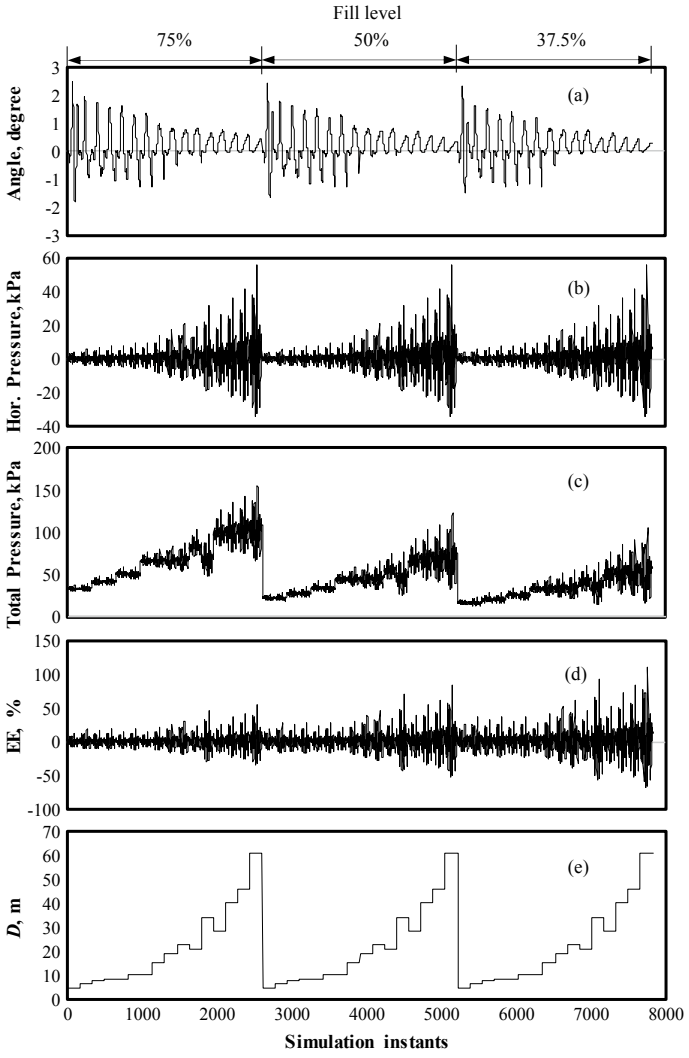

Fig. 11 Sequence of simulation outputs for the full set of conditions

– The horizontal, earthquake-related pressure, is a fraction of the total pressure (parts (b) and (c), Fig. 11).
– There is a wide variation of the earthquake effect (EE), with a maximum value of 112%, attained in the case of the larger diameter and smaller heights h (parts of Fig. 12).

However, a complementary analysis of the earthquake effect on the magnitude of the pressures at the bottom of the tank is necessary, in order to estimate the effect of the liquid sloshing on the integrity of the tank's material. That is, the 112% earthquake

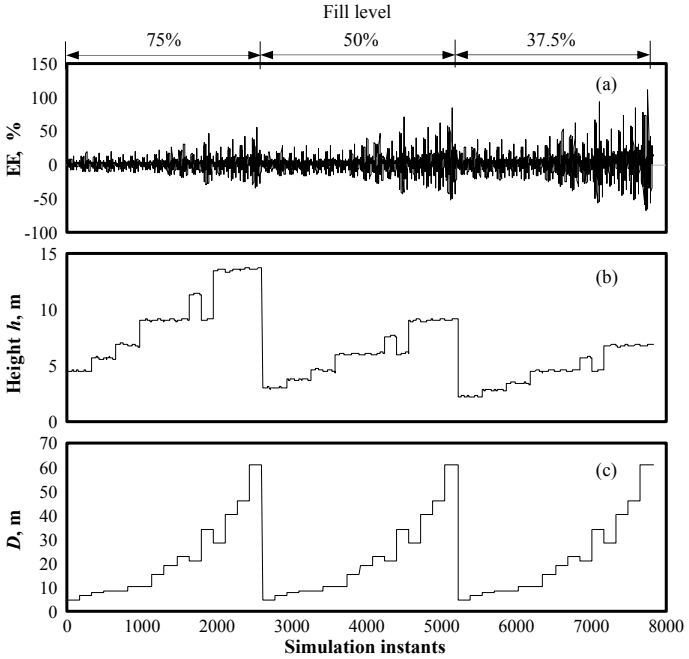

Fig. 12 Simulation outputs as a sequence of the 5 s response to perturbation

effect obtained above for the full combination of simulating conditions, would not necessarily involve a damage to the tank's material, as the situation involved low fill levels. An analysis is thus necessary, contemplating only the higher fill levels. Figure 13 illustrates the earthquake effect for the 75% fill level condition. In this case, the maximum value for the earthquake effect is 56.65%, also for the 67.5 m—diameter tank, but loaded at such fill level. This effect would be greater that considering the fully loaded conditions for this tank. Such magnitude for the earthquake effect has been also found when the overpressure is considered in the static analysis of the stresses in the tank's shell. Figure 14 describes the von Misses stresses in a half filled 10.43 m-diameter tank having a 10 mm thickness, when subjected to a lateral acceleration of 1.2 m/s^2.

6 Conclusions

A simplified approach for calculating the vertical and the horizontal pressures developed at the bottom of a cylindrical vertical tank when subjected to horizontal earthquake-related accelerations has been proposed in this paper. The core of the formulation consists of using the simple pendulum concept to simulate the sloshing angle of the liquid, where the length of the pendulum is set according to a validated

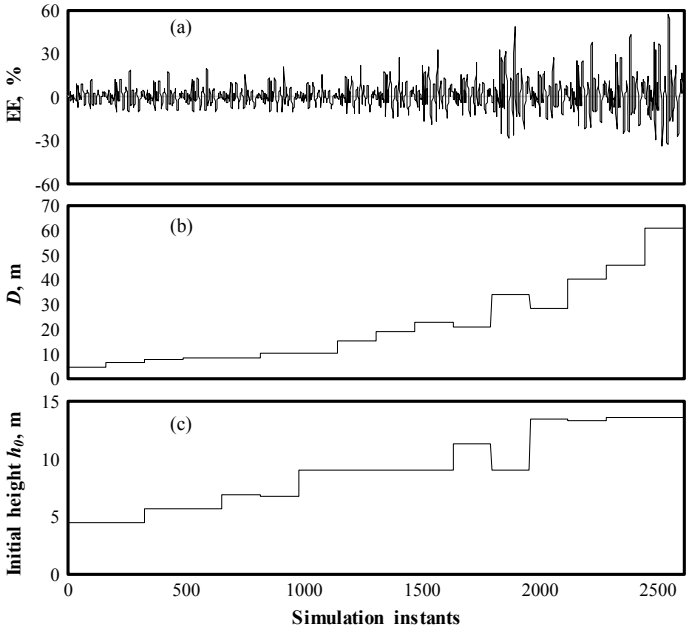

Fig. 13 Simulation outputs as a sequence of the 5 s response to perturbation, for the 75% fill level

methodology, which is described and experimentally verified in this research. The resulting total pressure thus depends on the following: liquid's density, the instantaneous vertical height of the liquid free surface, the tank's diameter, the gravity acceleration and the input horizontal acceleration. Estimations made for the pressures developed at the bottom of partially filled full-scale tanks, suggest a combined effect of about 50% above the nominal pressure. Such increase should be considered when designing tanks of large diameter (about 50 m) that could be potentially subjected to earthquake-related horizontal accelerations.

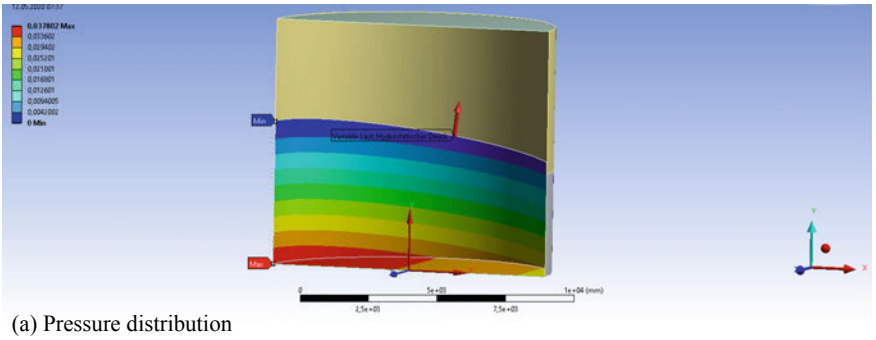

(a) Pressure distribution

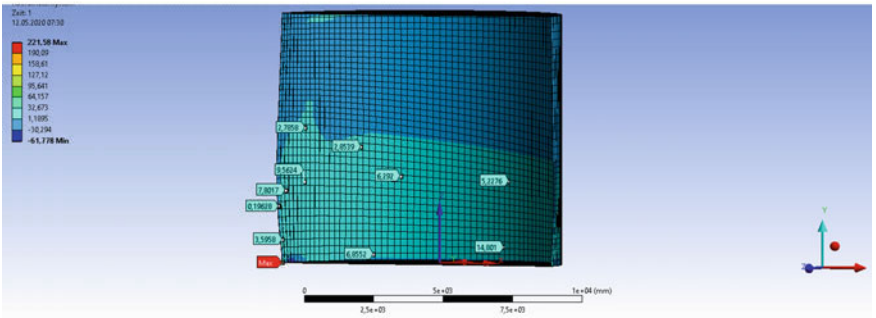

(b) Stress analysis.

Fig. 14 FEM calculations for a 10 mm thickness, 10.43 m-diameter tank, when subjected to a lateral acceleration of 1.2 m/s^2

References

1. Razaghi R, Sharavi M, Feizi MM (2015) Investigating the effect of sloshing on the energy absorption of tank wagons crash. Trans Can Soc Mech Eng 39(2):187–200
2. UDDC (1968) Hydraulic research in the United States. National Bureau of Standards, Washington, D.C., p 682
3. Bruno Faruolo L, Castro Pinto FAN (2015) Analysis of weigh-in-motion tank vehicles transporting liquid cargo on highways. IML Bull LVI(1):8–19
4. Matsui T, Uematsu Y, Kondo K, Wakasa T, Nagaya T (2009) Wind effects on sloshing of a floating roof in a cylindrical liquid storage tank. In: Proceedings of the ASME 2008 pressure vessels and piping conference. Volume 4: Fluid-structure interaction, Chicago, Illinois, USA, July 27–31, pp 401–410. ASME. https://doi.org/10.1115/PVP2008-61688
5. Kotrasová K, Kormaníková E (2017) Liquid storage cylindrical tank—earthquake analysis. In: Proceedings MATEC web conferences, vol 125
6. Kang T-W, Yang H-I, Jeon J-S (2019) Earthquake-induced sloshing effects on the hydrodynamic pressure response of rigid cylindrical liquid storage tanks using CFD simulation. Eng Struct 197(15):109376
7. Gaudarzi MA, Sabbagh-Yazdi E-R, Marx W (2010) Seismic analysis of hydrodynamic sloshing force on storage tank roofs. Earthq Spectra 26(1)
8. Malhotra PK (2006) Earthquake induces sloshing in tanks with insufficient freeboard. Struct Eng Int 16(3):222–225